THE JOURNAL OF PHYSICAL CHEMISTRY B

Article

pubs.acs.org/JPCB

# Kinetics of Photon Upconversion in Ionic Liquids: Time-Resolved Analysis of Delayed Fluorescence

Yoichi Murakami,*[,†] Hitomi Kikuchi,[‡,§] and Akio Kawai[‡]

[†]Global Edge Institute and [‡]Department of Chemistry, Graduate School of Science and Engineering, Tokyo Institute of Technology, 2-12-1 Ookayama, Meguro-ku, Tokyo, Japan

Supporting Information

**ABSTRACT:** Photon upconversion (UC) based on triplet−triplet annihilation (TTA) is an emerging wavelength shifting technology, which is applicable to sunlight. Previously we found that the quantum efficiency of TTA-UC ($\Phi_{UC}$) carried out in ionic liquids (ILs) is dependent on the type of IL employed. In this article we investigate the kinetics of the triplet emitter molecules (perylene) that implement TTA to determine the origin of the IL dependence of $\Phi_{UC}$. We measure the time-resolved delayed UC fluorescence intensities from samples made with five imidazolium-based ILs, and their intensity decay curves are analyzed with an analytical model. Consequently, several important aspects regarding both the first-order and second-order decays are elucidated. It is revealed that the IL dependence of $\Phi_{UC}$ primarily originates from the IL dependence of the branching ratio toward TTA upon an encounter of two triplet emitter molecules. Additionally, a strong correlation between the viscosity of the ILs and the branching ratios toward TTA is found. This finding is supported by temperature-dependent measurements, from which $\Phi_{UC}$ is found to be significantly affected by the viscosity of the IL. The results of this study should provide a clue for further improving $\Phi_{UC}$.

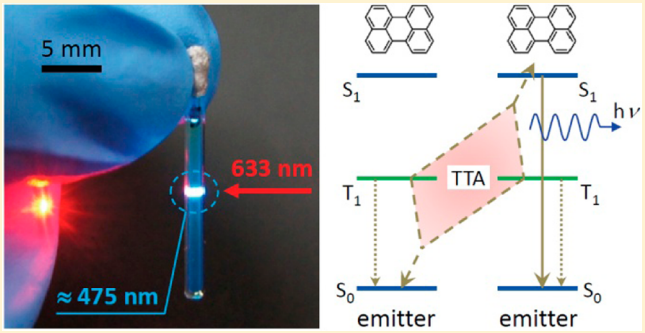


## INTRODUCTION

Photon upconversion (UC) is a wavelength-shifting technology in which two lower energy photons are combined to generate a higher energy photon. Recently, UC based on triplet−triplet annihilation (TTA) has been actively investigated[1−4] owing to the marked advantage of its applicability to low-intensity noncoherent sunlight,[1] making this technology promising to solar applications such as photovoltaics, photocatalysts, and photosynthesis.

UC based on TTA (TTA-UC) is achieved by utilizing two kinds of molecules: one type of molecule that performs triplet sensitization (the "sensitizer") and the other molecule that performs TTA and emission of an upconverted photon (the "emitter"). In TTA-UC, as shown by Scheme 1, the ground state ($S_0$) sensitizer molecules first absorb lower energy photons ($h\nu_1$) and are excited into the lowest-excited singlet ($S_1$) state, which immediately undergoes intersystem crossing (ISC) to the lowest-excited triplet ($T_1$) state. This triplet energy is then transferred to an emitter molecule based on an electron-exchanging mechanism (triplet energy transfer, TET).[5,6] Furthermore, upon the encounter of two $T_1$ emitter molecules, TTA ($T_1 + T_1 \rightarrow S_1 + S_0$) or triplet quenching ($T_1 + T_1 \rightarrow T_1 + S_0$ or $S_0 + S_0$) may occur. In this article, we use the term "TTA" solely for the former that gives rise to $S_1$ and $S_0$ based on the definition in ref 5. When the encountered pair ends in TTA, one of them becomes the $S_1$ state, from which a blue-shifted photon ($h\nu_2$) is emitted as delayed fluorescence. Because both TET and TTA processes are based on the electron-exchange mechanism that requires intermolecular collision,[5,6] the host medium must allow for diffusion of the molecules to achieve a meaningful UC quantum efficiency ($\Phi_{UC}$). Our definition of $\Phi_{UC}$ is so that it is unity when one upconverted photon is generated upon absorption of two photons ($0 \leq \Phi_{UC} \leq 1$).

Recently, we developed photon upconverters that employ ionic liquids (ILs) for the host medium.[7] ILs are novel room-temperature molten salts that possess negligibly small vapor pressures[8] and high thermal stabilities.[9] Because of their unique properties, ILs have recently been considered for many applications.[10] In addition to the nonflammability, the negligible vapor pressure (nonvolatility) is especially advantageous for the purpose of TTA-UC. This aspect allows samples to be thoroughly degassed under ultrahigh-vacuum (around $10^{-5}$ Pa),[7] giving rise to an efficient removal of dioxygen molecules that would otherwise act as a triplet quencher and cause sample degradation.

While the developed photon converters possess aforementioned advantages for application, there remains an unresolved matter: It has been found that the magnitude of $\Phi_{UC}$ is dependent on the type of IL employed.[7] At least for the five ILs

**Received:** February 10, 2013
**Revised:** March 23, 2013
**Published:** March 27, 2013

**Scheme 1. Qualitative Energy Level Diagram of Upconversion Process between $PdPh_4TBP$ and Perylene[a]**

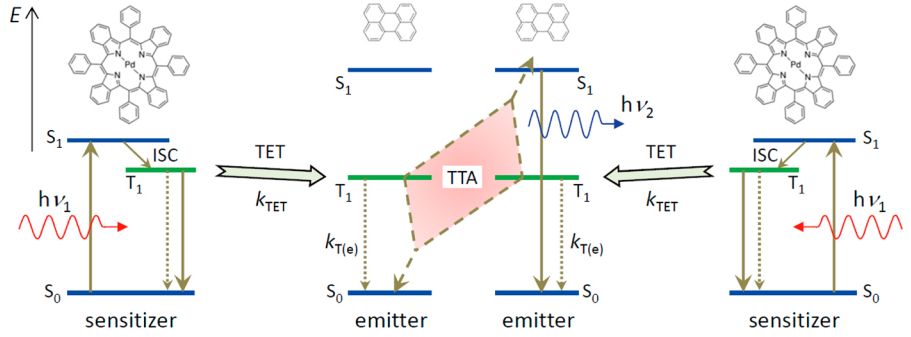


[a]ISC: intersystem crossing, TET: triplet energy transfer.

that are employed in this article, it has been confirmed that this IL-dependent $\Phi_{UC}$ is not due to extrinsic factors such as residual dioxygen or other types of quenchers, which should influence the first-order lifetime of the triplet states in an inconsistent or irreproducible manner. We have observed systematic and reproducible lifetimes of the emitter triplets in those ILs, as shown below.

Therefore, to establish a guideline to further increase $\Phi_{UC}$, the mechanism of this IL dependence needs to be elucidated. From our previous kinetics study[11] that investigated the TET process between the sensitizer and emitter molecules (for the same ILs as those employed in this article), the quantum efficiency for this process ($\Phi_{TET}$) was found to be independent of the ILs. Hence the IL-dependent $\Phi_{UC}$ should originate from the kinetics of the triplet emitter molecules that implement the TTA process. In this article, to address the above question, we investigate the kinetics of the emitter molecules by means of time-resolved photoemission experiments and their analyses.

So far, detailed kinetics studies of TTA-UC have been limited.[12,13] In previous studies the investigations were carried out under a fixed solvent of toluene,[12,13] and no detailed kinetics studies have been performed for the dependence on the media fluid employed. This provides further motivation to undertake this present study in addition to the aforementioned necessity to elucidate the kinetics of TTA-UC in ILs.

**Chart 1. Molecular Structures of (a) $PdPh_4TBP$, (b) Perylene, (c) Ionic Liquid Cation, and (d) Ionic Liquid Anion**

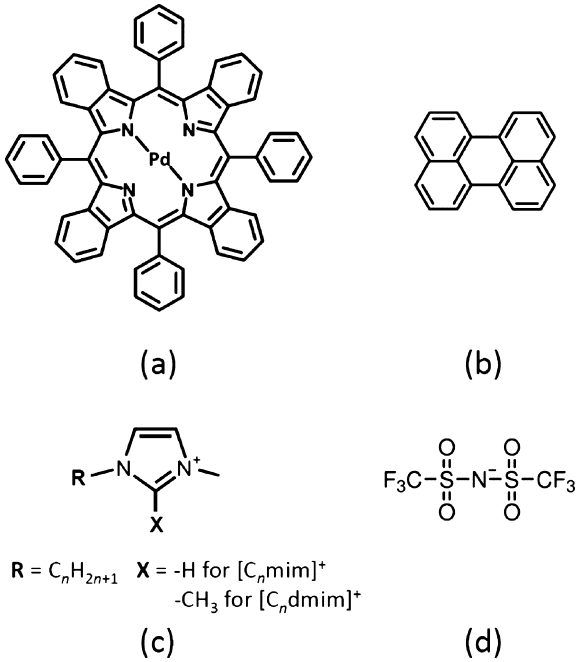


## EXPERIMENTAL SECTION

Chart 1 shows the structures of the molecules used in this article. In the chart, (a) and (b) are the sensitizer (Pd-tetraphenyltetrabenzoporphyrin, $PdPh_4TBP$) and emitter (perylene) molecules, while (c) and (d) are the cation ($[C_nmim]^+$, $[C_ndmim]^+$) and anion ($[NTf_2]^-$) of ILs, respectively. We employ five ILs in this article, $[C_nmim][NTf_2]$ (with $n$ = 2, 4, 6, or 8) and $[C_4dmim][NTf_2]$, where $[C_nmim]$: 1-alkyl-3-methylimidazolium, $[C_4dmim]$: 1-butyl-2,3-dimethylimidazolium, and $[NTf_2]$: bis(trifluoromethylsulfonyl)amide. All of the ILs were purchased from IoLiTec and stored under nitrogen. $PdPh_4TBP$ and perylene were purchased from Frontier Scientific and Sigma-Aldrich, respectively. All of the ILs were dried at 120 °C under vacuum for 4 h before use. The viscosities of the vacuum-dried ILs were measured by a cone–plate rheometer with a thermoelectric temperature controlled stage (Brookfield, R/S Plus) at 20 ± 0.2 °C.

The photoemission measurements were conducted with a home-built setup that consists of an optical parametric oscillator (OPO, EKSPLA NT-242), a monochromator (Princeton SP-2300), an arrayed CCD (Princeton PIX-IS:100BR), and a photomultiplier tube (Hamamatsu H11461-03). The details of the setup are shown in Figure S1 of the Supporting Information (SI). The OPO was operated at 630 nm, 10 Hz, and the pulse duration was 4 ns. The beam spot diameter at the sample position was 0.8 mm (Figure S2 in the SI). The time-resolved UC emission intensities were measured with the photomultiplier tube placed after the monochromator. Quantitative measurements of the emission intensities were performed using the CCD by integrating the spectrum for a much longer time than the OPO pulse period.

The temperature-dependent measurement of the UC emission intensity was done under ultrahigh vacuum in a microscopy cryostat (CIA, CFM-1738-102) with a temperature controlling unit. The cryostat was rigidly held horizontally under an objective lens of an optical microscope (Olympus, BX51M). The sample liquid (110 $\mu$L) was placed on a purpose-made sapphire dish that was adhered onto the coldfinger using ultrahigh-vacuum grease. Both the photoexcitation and fluorescence collection were through the objective lens. The excitation light source for this experiment was a continuous-


dx.doi.org/10.1021/jp401474n | J. Phys. Chem. B 2013, 117, 5180–5187

wave (CW) laser at 632.8 nm. The excitation laser beam was intentionally defocused on the sample, while the focus of the fluorescence collection path was adjusted so that the focal point comes slightly below the liquid surface. The fluorescence was fed into the monochromator through an optical fiber and measured by the CCD.

The sample preparation procedure was the same as in our previous report.[7] In brief, $PdPh_4TBP$ and perylene were dissolved in an IL with an intermediary of toluene, followed by vacuum pumping to remove toluene and dioxygen molecules (by an oil-free scroll pump and by a turbo-molecular pump, respectively). The liquid was then sealed in a square quartz tube with an inner dimension of 1 mm × 1 mm (Figure S2 in the SI). The concentrations of the sensitizer ($PdPh_4TBP$) and the emitter (perylene) in the samples were $1 \times 10^{-5}$ and $3 \times 10^{-3}$ M, respectively, unless otherwise specified.

The basic photoemission and absorption characteristics of the sample are shown here. Figure 1 shows the emission

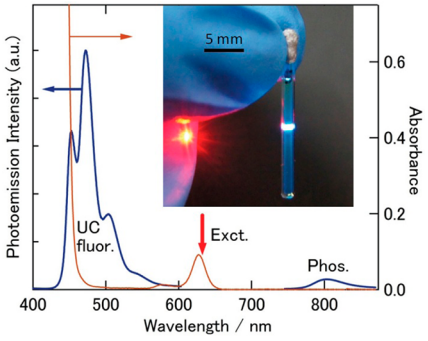


**Figure 1.** Photoemission spectrum (thick curve) upon excitation at 632.8 nm (arrow) and the optical absorption spectrum (thin curve, path length = 1 mm). Inset: A sample made with $[C_6mim][NTf_2]$ sealed in the 1 mm × 1 mm square quartz tube, upconverting red light (632.8 nm, ca. 2 W/cm$^2$) into blue emission. This sample was fabricated on December 18, 2010 and left in the air since then. This photograph was taken on January 28, 2013.

spectrum upon excitation at 632.8 nm measured from the typical sample. The feature at ~475 nm is delayed UC fluorescence from perylene, and the feature at ~800 nm is phosphorescence from $PdPh_4TBP$. This Figure also shows the optical absorption spectrum, where the absorption around 630 nm is the Q-band of $PdPh_4TBP$ and the absorption for <470 nm is from both $PdPh_4TBP$ and perylene. The inset shows a photograph of a sample upconverting a red CW incident light (632.8 nm, ca. 2 W/cm$^2$) into blue emission. Because residual dioxygen concentration in the samples is suppressed by the aforementioned ultrahigh vacuum pumping, the samples usually continue to work for a long time, on the order of years.

In Figure 1, because there is a spectral overlap between the UC fluorescence and the optical absorption of $PdPh_4TBP$, there is a possibility of Förster resonant energy transfer (FRET) from $S_1$ perylene to $S_0$ $PdPh_4TBP$. However, the contribution of the FRET in the present system is estimated to be sufficiently low and is further described in detail in the SI.

## RESULTS AND DISCUSSION

**Excitation Pulse Intensity Dependence.** Figure 2a shows the normalized intensity decay curves of the delayed UC fluorescence at 475 nm measured with different excitation pulse intensities, denoted by $I_{exct}$. The shape changes with $I_{exct}$. Figure

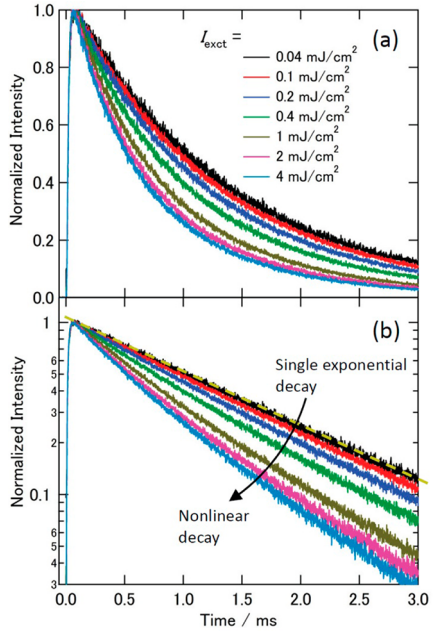


**Figure 2.** Normalized intensity decay curves of the delayed UC fluorescence at 475 nm upon pulse excitation at 630 nm, displayed in (a) linear and (b) logarithmic scales. The yellow dashed line is an eye-guide for single exponential decay. The IL was $[C_4dmim][NTf_2]$.

2b is the logarithmic presentation of the same data. For the lowest $I_{exct}$ (0.04 mJ/cm$^2$), a good fitting of the decay curve is given by a single-exponential decay function, but with increasing pulse intensity the decay curve can no longer be fit by a single-exponential function. This shape change is ascribed to an increased proportion of the second-order decay in the decays of the $T_1$ perylene population.

The formation process of $T_1$ perylene (i.e., rise of the UC fluorescence) as a result of TET from $T_1$ $PdPh_4TBP$, corresponding to the early time region of Figure 2, has been investigated and discussed in detail in our previous report.[11] The rise of the UC fluorescence along with the decay of the phosphorescence from $PdPh_4TPB$ (the kinetics shown in figure 2a of ref 11) that is pertinent to the present study is shown for three different perylene concentrations in Figure S3 of SI.

The filled circles in Figure 3a present the $I_{exct}$ dependence of the time-integrated UC fluorescence intensity, which shows saturation behavior. This UC intensity saturation is partially attributed to the photosaturation of the sensitizer molecule ($PdPh_4TBP$) upon pulse excitation, which is perceived by measuring the $I_{exct}$ dependence of the time-integrated phosphorescence intensity from $PdPh_4TBP$ (plotted to the left axis of Figure 3b). This photosaturation was reversible, which means that no permanent damage was caused in $PdPh_4TBP$.

Here we introduce the "saturation factor ($f_{sat}$)", which is defined as the ratio of the measured phosphorescence intensity from $PdPh_4TBP$ to the hypothetical intensity that was obtained by linearly extrapolating from the phosphorescence intensity at 0.04 mJ/cm$^2$ (where we assumed there is no photosaturation in $PdPh_4TBP$). This $f_{sat}$ was plotted to the right axis of Figure 3b. Then, the raw data in Figure 3a (filled circles) were divided by the $f_{sat}$ to generate the corrected data (open circles, Figure 3a). As exhibited by the corrected data points, the incremental exponent changes from 2 into 1 with increasing $I_{exct}$. This "2 to 1" transition in the exponent with $I_{exct}$ was observed and


dx.doi.org/10.1021/jp401474n | J. Phys. Chem. B 2013, 117, 5180−5187

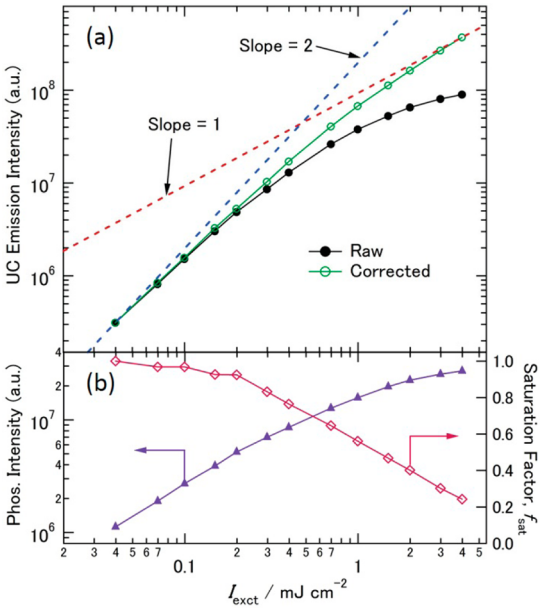


**Figure 3.** (a) Dependence of the UC fluorescence intensity at 475 nm on the excitation pulse intensity. The filled circles are raw data and the open circles are the data corrected by taking into account the $f_{sat}$ shown in the next panel. (b) Dependences of the phosphorescence intensity at 800 nm (triangle) and the saturation factor $f_{sat}$ (diamond) on the excitation pulse intensity. The sample employed for this Figure is identical to that employed for Figure 2. The excitation wavelength was 630 nm.

discussed in previous reports performed under CW[7] and femtosecond pulse excitation.[12] Similar to the interpretation in those previous studies,[7,12] the results shown in Figure 3a are interpreted as follows: The second-order decay of $T_1$ perylene is significant at $I_{exct}$ = 4 mJ/cm$^2$, which also agrees with the observed $I_{exct}$ dependence of the UC fluorescence decay curves in Figure 2.

**Analytical Model.** We employ a standard second-order rate equation[13−15]

$$\frac{d[T_1]_t}{dt} = G_{in}(t) - k_{T(e)}[T_1]_t - k_2[T_1]_t^2 \quad (1)$$

to describe the time dependence of the concentration of triplet perylene, denoted by $[T_1]_t$. In eq 1, $G_{in}(t)$ is the rate of creation of triple perylene at time $t$, $k_{T(e)}$ is the first-order decay rate, and $k_2$ is the rate of the second-order decay arising from all bimolecular pathways including TTA ($T_1 + T_1 \rightarrow S_1 + S_0$) and triplet quenching ($T_1 + T_1 \rightarrow T_1 + S_0$ or $S_0 + S_0$). Because the TET from $PdPh_4TBP$ to perylene after the pulse-excitation is completed within much shorter time scale (tens of microseconds)[11] than that of the delayed fluorescence decay (order of milliseconds, Figure 2), we approximate that the initial concentration of triplet perylene, $[T_1]_0$, is instantaneously established at $t$ = 0. In the following sections, we will discuss our experimental results based on an analytical framework introduced by Weisman and Bachilo,[14] which was recently applied to TTA-UC.[13] The solution to eq 1 is given by[13−15]

$$[T_1]_t = \left\{\left(\frac{1}{[T_1]_0} + \frac{k_2}{k_{T(e)}}\right)\exp(k_{T(e)}t) - \frac{k_2}{k_{T(e)}}\right\}^{-1} \quad (2)$$

We denote the rate of TTA by $k_{TTA}$, which is defined as

$$k_{TTA} = \varphi_S k_2 \quad (3)$$

Here $\varphi_S$ denotes the branching ratio for an encounter complex formed by two $T_1$ emitter molecules entering the singlet manifold to result in TTA. The basis and some important discussion about the branching ratio have been previously given.[12,13] With $k_{TTA}$ in eq 3, the intensity of UC fluorescence emission at time $t$, $I_{UC}(t)$, is expressed as

$$I_{UC}(t) = k_{TTA}[T_1]_t^2\Phi_F\zeta \propto k_{TTA}[T_1]_t^2 \quad (4)$$

where $\Phi_F$ and $\zeta$ denote the fluorescence quantum yield from $S_1$ perylene and the instrumental correction factor of the experimental system, respectively. The $\Phi_F$ has been confirmed to be the same for the five ILs employed in this study. Hereafter, we set $\Phi_F\zeta$ = 1 for analytical simplicity not only because the $\Phi_F\zeta$ is common in this article but also because normalized intensity decay curves are analyzed in this article. Then, a substitution of eq 2 into eq 4 yields

$$\Psi = \{(1 + \Omega)\exp(k_{T(e)}t) - \Omega\}^{-2} \quad (5)$$

where $\Psi$ ($0 \le \Psi \le 1$) and $\Omega$ ($\ge 0$) are the dimensionless variables that we introduced as

$$\Psi \equiv \frac{I_{UC}(t)}{k_{TTA}[T_1]_0^2} = \frac{[T_1]_t^2}{[T_1]_0^2}, \quad \Omega \equiv \frac{k_2[T_1]_0}{k_{T(e)}} \quad (6)$$

Here $\Psi$ represents the dimensionless intensity of UC fluorescence and $\Omega$ represents the ratio of the second-order decay to the first-order decay at $t$ = 0. From eq 2, the fraction of $[T_1]_0$ that decays by second-order processes, denoted by $f_2$, is given by[13]

$$f_2 = 1 - \frac{\ln(1 + \Omega)}{\Omega} \quad (7)$$

The UC fluorescence intensity decay curves shown in Figure 2 can be fit well by eq 5, as shown by Figure S4 in the SI. The validity of applying the above analytical model toward our experimental results has been confirmed, and the details are described in the SI.

**Ionic-Liquid-Dependent Kinetics of First-Order Decay.** Figure 4 shows the normalized intensity decay curves of the UC fluorescence at 475 nm from the samples made with the five ILs. All of the curves were obtained at $I_{exct}$ = 4 mJ/cm$^2$. The parameters $\Omega$ and $\tau_{T(e)}$ ($\equiv k_{T(e)}^{-1}$) were obtained from the fitting of eq 5 and are shown in Table 1. The results reveals a

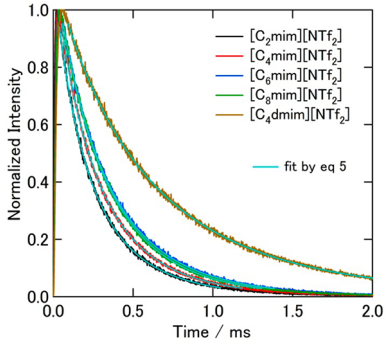


**Figure 4.** Time-resolved intensity decays of the UC fluorescence at 475 nm measured upon excitation at 630 nm for the samples made with the five ILs. The excitation pulse intensity was 4 mJ/cm$^2$ for all cases. The curves fit by eq 5 are also shown.


dx.doi.org/10.1021/jp401474n | J. Phys. Chem. B 2013, 117, 5180−5187

**Table 1. List of Parameters for the Five Experimental Cases**

| case no. | ionic liquid | $\Omega^a$ | $\tau_{T(e)}$/ms$^a$ | $\eta$/mPa s$^b$ | $f_2{}^c$ | $\Phi_{UC}{}^d$ | $\varphi_{S,\,relative}{}^e$ |
|---|---|---|---|---|---|---|---|
| 1 | $[C_2mim][NTf_2]$ | 1.2 | 0.87 | 38 | 0.33 | 0.033 | 0.29 |
| 2 | $[C_4mim][NTf_2]$ | 0.77 | 0.85 | 61 | 0.26 | 0.044 | 0.50 |
| 3 | $[C_6mim][NTf_2]$ | 0.66 | 0.95 | 88 | 0.23 | 0.052 | 0.66 |
| 4 | $[C_8mim][NTf_2]$ | 0.50 | 0.86 | 119 | 0.18 | 0.042 | 0.68 |
| 5 | $[C_4dmim][NTf_2]$ | 1.0 | 2.1 | 132 | 0.31 | 0.106 | 1* |

[a]From fitting of the decay curves in Figure 4. [b]Measured on ionic liquids without solute molecules at 20 ± 0.2 °C. [c]From eq 7. [d]Our previous data obtained with a CW light source (ref 7). [e]From eq 8, normalized relative to *. Definition of the symbols: Ω, the initial ratio of the second-order decay to the first-order decay (eq 6); $\tau_{T(e)}$, the first-order triplet lifetime of the emitter; $\eta$, ionic liquid viscosity; $f_2$, the fraction of initially created emitter triplets that decay by second-order processes (eq 7); $\Phi_{UC}$, upconversion quantum efficiency; $\varphi_S$, the branching ratio for an encounter complex of two $T_1$ emitter molecules to give rise to TTA (eq 3).

remarkable difference in $\tau_{T(e)}$ between the samples made with $[C_nmim][NTf_2]$ ($n$ = 2, 4, 6, 8) and the sample made with $[C_4dmim][NTf_2]$, showing a strong influence of IL cation on the first-order decay rate. The reproducibility of these results has been confirmed by repeating the same experiments. As shown by Chart 1, the difference between these ILs exists in the "X"-position of an imidazolium ring. Several previous studies[16−18] have pointed out that this position of $[C_nmim]^+$ cation serves as a "hydrogen bonding site." The site is considered to be weakened when the −H in this position is replaced by $-CH_3$ to form $[C_ndmim]^+$.[19] Although the exact effect of the hydrogen-bonding formation on the electronic properties of solute molecules in ILs is not yet clear, we tentatively attribute the shorter $\tau_{T(e)}$ found for the ILs with $[C_nmim]^+$ to the stronger perturbation toward the wave function of the triplet perylene caused by the hydrogen bonding interaction exerted from $[C_nmim]^+$ species.

**Ionic-Liquid-Dependent Kinetics of Second-Order Decay.** Next, the IL dependence of the second-order decay is inspected. The initial triplet concentration $[T_1]_0$ is considered to be the same for the five cases in Table 1 based on the following reasons: First, the experimental conditions ($I_{exct}$ and the molecular concentrations) were common among these cases. Second, the $\Phi_{TET}$ was found to be independent of those ILs.[11] Therefore, from $k_{T(e)}\Omega = k_2[T_1]_0$ (eq 6), we can assume $k_{T(e)}\Omega \propto k_2$ in Table 1.

Figure 5a shows the relationship between $k_{T(e)}\Omega$ ($\propto k_2$) and the inverse viscosity of the IL ($\eta^{-1}$). This tendency, that is, larger $\eta$ leads to smaller $k_2$, qualitatively agrees with our expectation. However, it is known that the diffusivities of solute molecules in different ILs generally do not linearly correlate with their bulk viscosities, as has been seen as deviations from the prediction by the Smoluchowski's theory based on the Stokes−Einstein relation.[20−22] In our previous study,[11] we determined the pseudo-first-order quenching rate constant of $T_1$ $PdPh_4TBP$ by $S_0$ perylene, denoted by $k_q$, for the same five ILs. Here we adopt the $k_q$ as a quantity that represents the actual molecular diffusivity in those ILs. Figure 5b plots the relationship between the $k_{T(e)}\Omega$ and $k_q$ for the five cases, which shows a linear correlation between the pseudo-first-order rate constant ($k_q$) and the second-order rate constant ($k_2$). This result indicates that there is no anomaly in $k_2$ among those ILs. Furthermore, we assume that the $k_q$ is a diffusion-controlled rate constant. With this assumption, the linear correlation found in Figure 5b strongly implies that the second-order processes (for $k_2$) also proceeds at a diffusion-controlled rate.

**Discussion on Ionic-Liquid-Dependent $\Phi_{UC}$.** The IL-dependent $\Phi_{UC}$ was found in our previous report[7] using a CW excitation light source. The sample preparation procedure as

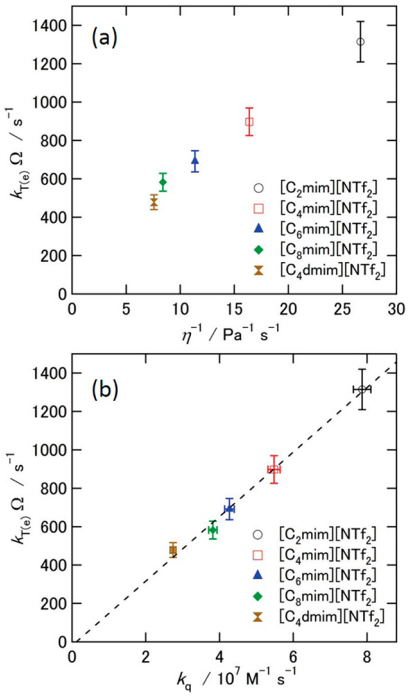


**Figure 5.** Dependences of $k_{T(e)}\Omega$ on (a) the inverse viscosity of the IL and (b) the quenching rate constant of $T_1$ $PdPh_4TBP$ by $S_0$ perylene determined in ref 11. The dashed line is the least-squares line fit to the five data points. Error bars are ±8% and ±3% for $k_{T(e)}\Omega$ and $k_q$, respectively.

well as the molecular concentrations of $PdPh_4TBP$ and perylene in ref 7 was the same as those in this present article. The values of the previously measured $\Phi_{UC}$ for the five ILs are shown in Table 1. Below, using this information, we will inspect the factor that principally influences $\Phi_{UC}$ in the present system. The employment of the $\Phi_{UC}$ obtained with the CW excitation light source for discussing the present results is justified because both the $\Phi_{UC}$ in ref 7 (measured at the excitation intensity of ~6 W/cm$^2$) and the decay curves in Figure 4 (measured at $I_{exct}$ = 4 mJ/cm$^2$) were measured in the "slope =1" region (see Figure 3a in this article and figure 3a in ref 7), that is, both under the situation where the magnitudes of $\Phi_{UC}$ were saturated.

Because $\Phi_{TET}$ is common among those five samples as mentioned above, the relationship "$\Phi_{UC} \propto \tilde{I}_{UC}/[T_1]_0$" holds. Here, $\tilde{I}_{UC}$ denotes the time-integrated UC fluorescence intensity per one excitation pulse input, defined by eq S1 (in the SI). With eq 3, eq 6, and eq S2 (in the SI), this relationship is rewritten as


dx.doi.org/10.1021/jp401474n | J. Phys. Chem. B 2013, 117, 5180−5187

$$\Phi_{UC} \propto \varphi_S f_2 \Leftrightarrow \varphi_S \propto \Phi_{UC} f_2^{-1} \quad (8)$$

By using the second form of eq 8, we can examine the variance of $\varphi_S$ among the five cases in Table 1. The obtained $\varphi_{S,relative}$, which is the value normalized relative to the case of $[C_4dmim][NTf_2]$, is shown in the rightmost column. This reveals an existence of a remarkable variance in the magnitude of $\varphi_S$ depending on the ILs. It is noted that for this purpose we did not use the previously employed method[12] in which the intensities of the prompt and delayed UC fluorescence from a same sample are compared, because this method gives rise to a large error in our experimental system due to the remarkable difference in their emission-ray paths to the entrance slit of the monochromator caused by the large difference between the concentrations of the sensitizer and emitter molecules (1:300).

Summarizing the findings obtained above, the IL dependence of $\Phi_{UC}$ is described as follows, which is depicted in Scheme 2.

**Scheme 2. Schematic Depiction for How $\Phi_{UC}$ Is Affected by Relevant Parameters**

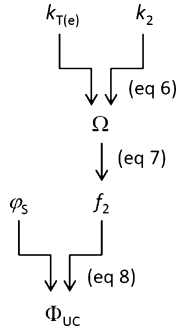


$\Phi_{UC}$ is directly affected by two parameters, $\varphi_S$ and $f_2$ (eq 8). Here $f_2$ is a monotonically increasing function of only Ω (eq 7, see also the inset of Figure S5 in the SI). Ω is proportional to the ratio $k_2/k_{T(e)}$ (eq 6). Therefore, smaller $k_{T(e)}$, as well as larger $k_2$, contributes to higher $\Phi_{UC}$. As mentioned in the previous paragraph, the IL-dependent variance of $\varphi_S$ is large. Altogether, the difference of the two extreme cases in Table 1, $[C_2mim][NTf_2]$ ($\Phi_{UC} \approx 0.03$) and $[C_4dmim][NTf_2]$ ($\Phi_{UC} \approx 0.1$), is described as follows: First, in the case of $[C_4dmim][NTf_2]$, the smaller $k_{T(e)}$ results in a larger Ω (eq 6) and hence a larger $f_2$ (eq 7). This larger $f_2$ *and* the larger $\varphi_S$ (Table 1) give rise to a higher $\Phi_{UC}$ (eq 8). In contrast, in the case of $[C_2mim][NTf_2]$, it has the lowest $\eta$ among the ILs tested, resulting in the largest $k_2$ (Figure 5). This feature compensates its disadvantage of the larger $k_{T(e)}$, resulting in the similarly large Ω (eq 6) and hence $f_2$ (eq 7). However, this IL shows a much smaller $\varphi_S$ (Table 1), and this aspect eventually gives rise to the smaller $\Phi_{UC}$ (eq 8). Therefore, it is concluded that the IL dependence of $\Phi_{UC}$ in the present system principally originates from the IL dependence of the branching ratio for the TTA manifold ($\varphi_S$), although the IL dependence of $\tau_{T(e)}$ also contributes to the magnitude of $\Phi_{UC}$.

Furthermore, the results of the analysis (Table 1) have unveiled an important aspect regarding $\varphi_S$; that is, the higher $\eta$ leads to the higher $\varphi_S$. To confirm and support this finding that was derived from the five samples, we have carried out the following temperature-dependent measurement of the UC emission intensity from one identical sample, whose result is shown in Figure 6. In this experiment, the IL was $[C_4mim][NTf_2]$, $[PdPh_4TBP] = 1 \times 10^{-5}$ M, and $[perylene] = 1 \times 10^{-3}$ M, and the measurement was done in a temperature-controlled cryostat as described in the Experimental Section. The vertical axis represents spectrally integrated emission intensity. The temperature of fusion for $[C_4mim][NTf_2]$ has been reported to be −3 °C,[23] and hence the sample was in the liquid state for the entire temperature range of Figure 6. The temperature dependence of the viscosity of this IL has been reported in detail in ref 24. As shown by the Figure, a remarkable increase in the UC emission intensity was observed upon cooling from 30 to 0 °C while the viscosity of this ionic liquid increased significantly (ca. a factor of 5)[24] for this temperature range. It is noted that the remarkable increase in the UC emission intensity over this temperature range (opposing the factor of ca. 5 increase in the viscosity) cannot be attributed to the temperature dependence of the triplet lifetime, because the thermal energy difference between 30 and 0 °C is small (~2.6 meV). It is also noted that the magnitude of IL viscosity itself does not influence the triplet lifetime, as can be recognized by comparing $\tau_{T(e)}$ for the case nos. 1−4 in Table 1. The entire measured temperature range (−60 to 50 °C) of the data for Figure 6 is shown in Figure S6 in the SI.

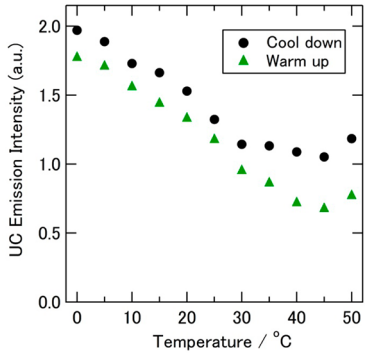


**Figure 6.** Temperature dependence of the spectrally integrated UC emission intensity measured upon CW excitation at 632.8 nm. The sample was made with $[C_4mim][NTf_2]$ and set inside an ultrahigh-vacuum cryostat. The experiment started at 50 °C, then cooled (circles, to −60 °C; see Figure S6 in the SI) and warmed to 50 °C again (triangles). The sample amount was 110 μL. The time interval of 5 to 15 min was taken between the adjacent data points.

Finally, we remark on the observed viscosity dependence, although here we limit ourselves to a preliminary hypothesis for further studies. In general, the higher solvent viscosity leads to a slower rotational motion of solute molecules, as recognized by the formula of Stokes−Einstein−Debye equation.[25,26] We hypothesize that the reduction in the rotational motion of the triplet molecules enhances $\varphi_S$. This attribution is based on the fact that the reduction of the *translational* diffusivity (i.e., reduction of $k_2$) is harmful to $\Phi_{UC}$ because it lowers Ω (by eq 6). This viewpoint leads to a possible explanation of the higher $\varphi_S$ observed for the sample made with $[C_4dmim][NTf_2]$, as compared with $[C_8mim][NTf_2]$ that has similar viscosity (see Table 1), which may be due to the lowered entropy of this IL: A previous theoretical study[19] that investigated $[C_4dmim][NTf_2]$ has pointed out that the methylation of the "X"-position in an imidazolium cation (see Chart 1) causes (i) a steric hindrance toward the motion of the alkyl chain next to it and (ii) a reduction in the number of stable anion interaction sites, and has concluded that both of these factors, (i) and (ii), should give rise to significant reduction of the entropy (and an increase in the microscopic order) of this particular IL. However, further discussion on this hypothesis is beyond the


dx.doi.org/10.1021/jp401474n | J. Phys. Chem. B 2013, 117, 5180−5187

scope of this article. We are planning to set up an experimental system for this purpose, which will be reported elsewhere in the future.

## CONCLUSIONS

We have investigated the kinetics of the triplet emitter molecules that implement the TTA process to clarify the mechanism of the IL-dependent UC quantum efficiency ($\Phi_{UC}$). The investigations were performed by the time-resolved measurements of the delayed UC fluorescence intensities from the samples made with the five ILs and by the analysis of the obtained intensity decay curves using the model introduced. The validity of applying this model to the present experimental results has been confirmed (Figure S5 in the SI). Consequently, several important aspects regarding both the first-order and second-order decays of triplet emitters were elucidated. For the first-order decay, the triplet emitter lifetime ($\tau_{T(e)}$) has been found to be highly dependent on the cation of ILs (Table 1). Namely, the existence of a hydrogen bonding site negatively impacts $\Phi_{UC}$ by causing a lowering of $\tau_{T(e)}$. As for the second-order decay, no IL-dependent anomaly was found in the magnitude of $k_2$ (Figure 5b). In addition, the second-order decays in the present system have been implied to proceed at a diffusion-controlled rate.

Further from the analysis, it has been revealed that the IL dependence of $\Phi_{UC}$ primarily originates from the IL dependence of the branching ratio toward TTA ($\varphi_S$). Additionally, a correlation between the IL viscosity and $\varphi_S$ was found (Table 1). This indicates that the viscosity is an important factor that influences $\varphi_S$ and hence $\Phi_{UC}$. This finding was corroborated by a supporting experiment where the temperature-dependent UC emission intensity was measured from one identical sample (Figure 6). These findings should provide a useful strategy for increasing the efficiency of TTA-UC.

## ASSOCIATED CONTENT

### Supporting Information

Details of the measurement setup, OPO laser beam profile at the sample position, dimension of the sample tube, evaluation of Förster resonant energy transfer, rise of UC fluorescence intensity at three different perylene concentrations, results of the fitting by eq 5 to the UC fluorescence decay curves shown in Figure 2, table that summarizes the parameters obtained by the fitting, confirmation of the validity of the employed model, and the results of Figure 6 shown for the entire measured temperature range. This material is available free of charge via the Internet at http://pubs.acs.org.

## AUTHOR INFORMATION

### Corresponding Author

*E-mail: murakami.y.af@m.titech.ac.jp.

### Present Address

[§]Hitomi Kikuchi: NEC Soft Ltd., 2-3-3 minatomirai, Nishi-ku, Yokohama, Kanagawa 220-6113, Japan.

### Notes

The authors declare no competing financial interest.

## ACKNOWLEDGMENTS

This work was supported by Grant-in-Aid for Young Scientists A (no. 23686035) and Grant-in-Aid for Scientific Research (no. 24350004) from the Ministry of Education, Culture, Sports, Science and Technology (MEXT), Japan. We thank Ryan Gresback of Tokyo Inst. Tech. for the refinement of English and expressions.

## REFERENCES

(1) Baluschev, S.; Miteva, T.; Yakutkin, V.; Nelles, G.; Yasuda, A.; Wegner, G. Up-Conversion Fluorescence: Noncoherent Excitation by Sunlight. *Phys. Rev. Lett.* **2006**, *97*, 143903-1−143903-3.

(2) Singh-Rachford, T. N.; Castellano, F. N. Photon Upconversion Based on Sensitized Triplet−Triplet Annihilation. *Coord. Chem. Rev.* **2010**, *254*, 2560−2573.

(3) Cheng, Y. Y.; Fückel, B.; MacQueen, R. W.; Khoury, T.; Clady, R. G. C. R.; Schulze, T. F.; Ekins-Daukes, N. J.; Crossley, M. J.; Stannowski, B.; Lips, K.; et al. Improving the Light-Harvesting of Amorphous Silicon Solar Cells with Photochemical Upconversion. *Energy Environ. Sci.* **2012**, *5*, 6953−6959.

(4) Turshatov, A.; Busko, D.; Avlasevich, Y.; Miteva, T.; Landfester, K.; Baluschev, S. Synergetic Effect in Triplet−Triplet Annihilation Upconversion: Highly Efficient Multi-Chromophore Emitter. *Chem. Phys. Chem.* **2012**, *13*, 3112−3115.

(5) Turro, N. J.; Ramamurthy, V.; Scaiano, J. C. *Principles of Molecular Photochemistry*; University Science Books: Sausalito, CA, 2009.

(6) Monguzzi, A.; Tubino, R.; Meinardi, F. Upconversion-Induced Delayed Fluorescence in Multicomponent Organic Systems: Role of Dexter Energy Transfer. *Phys. Rev. B.* **2008**, *77*, 155122-1−155122-4.

(7) Murakami, Y. Photochemical Photon Upconverters with Ionic Liquids. *Chem. Phys. Lett.* **2011**, *516*, 56−61.

(8) Zaitsau, D. H.; Kabo, G. J.; Strechan, A. A.; Paulechka, Y. U.; Tschersich, A.; Verevkin, S. P.; Heintz, A. Experimental Vapor Pressures of 1-Alkyl-3-methylimidazolium Bis-(trifluoromethylsulfonyl)imides and a Correlation Scheme for Estimation of Vaporization Enthalpies of Ionic Liquids. *J. Phys. Chem. A.* **2006**, *110*, 7303−7306.

(9) Ngo, H. L.; LeCompte, K.; Hargens, L.; McEwen, A. B. Thermal Properties of Imidazolium Ionic Liquids. *Thermochim. Acta.* **2000**, *357*, 97−102.

(10) Plechkova, N. V.; Seddon, K. R. Applications of Ionic Liquids in the Chemical Industry. *Chem. Soc. Rev.* **2008**, *37*, 123−150.

(11) Murakami, Y.; Kikuchi, H.; Kawai, A. Kinetics of Photon Upconversion in Ionic Liquids: Energy Transfer between Sensitizer and Emitter Molecules. *J. Phys. Chem. B.* **2013**, *117*, 2487−2494.

(12) Cheng, Y. Y.; Khoury, T.; Clady, R. G. C. R.; Tayebjee, M. J. Y.; Ekins-Daukes, N. J.; Crossley, M. J.; Schmidt, T. W. On the Efficiency Limit of Triplet−Triplet Annihilation for Photochemical Upconversion. *Phys. Chem. Chem. Phys.* **2010**, *12*, 66−71.

(13) Cheng, Y. Y.; Fückel, B.; Khoury, T.; Clady, R. G. C. R.; Tayebjee, M. J. Y.; Ekins-Daukes, N. J.; Crossley, M. J.; Schmidt, T. W. Kinetic Analysis of Photochemical Upconversion by Triplet-Triplet Annihilation: Beyond Any Spin Statistical Limit. *J. Phys. Chem. Lett.* **2010**, *1*, 1795−1799.

(14) Bachilo, S. M.; Weisman, R. B. Determination of Triplet Quantum Yields from Triplet-Triplet Annihilation Fluorescence. *J. Phys. Chem. A.* **2000**, *104*, 7711−7714.

(15) Murakami, Y.; Kono, J. Existence of an Upper Limit on the Density of Excitons in Carbon Nanotubes by Diffusion-Limited Exciton-Exciton Annihilation: Experiment and Theory. *Phys. Rev. B.* **2009**, *80*, 035432-1−035432-10.

(16) Hardacre, C.; Holbrey, J. D.; McMath, S. E. J.; Bowron, D. T.; Soper, A. K. Structure of Molten 1,3-Dimethylimidazolium Chloride Using Neutron Diffraction. *J. Chem. Phys.* **2003**, *118*, 273−278.

(17) Talaty, E. R.; Raja, S.; Storhaug, V. J.; Dölle, A.; Carper, W. R. Raman. and Infrared Spectra and ab Initio Calculations of $C_{2-4}$MIM Imidazolium Hexafluorophosphate Ionic Liquids. *J. Phys. Chem. B.* **2004**, *108*, 13177−13184.

(18) Dong, K.; Zhang, S.; Wang, D.; Yao, X. Hydrogen Bonds in Imidazolium Ionic Liquids. *J. Phys. Chem. A.* **2006**, *110*, 9775−9782.

(19) Hunt, P. A. Why Does a Reduction in Hydrogen Bonding Lead to an Increase in Viscosity for the 1-Butyl-2,3-dimethyl-imidazolium-Based Ionic Liquids? *J. Phys. Chem. B.* **2007**, *111*, 4844−4853.

(20) McLean, A. J.; Muldoon, M. J.; Gordon, C. M.; Dunkin, I. R. Bimolecular Rate Constants for Diffusion in Ionic Liquids. *Chem. Commun.* **2002**, *17*, 1880−1881.
(21) Skrzypczak, A.; Neta, P. Diffusion-Controlled Electron-Transfer Reactions in Ionic Liquids. *J. Phys. Chem. A.* **2003**, *107*, 7800−7803.
(22) Nishiyama, Y.; Fukuda, M.; Terazima, M.; Kimura, Y. Study of the Translational Diffusion of the Benzophenone Ketyl Radical in Comparison with Stable Molecules in Room Temperature Ionic Liquids by Transient Grating Spectroscopy. *J. Chem. Phys.* **2008**, *128*, 164514-1−164514-9.
(23) Blokhin, A. V.; Paulechka, Y. U.; Strechan, A. A.; Kabo, G. J. Physicochemical Properties, Structure, and Conformations of 1-Butyl-3-methylimidazolium Bis(trifluoromethanesulfonyl)imide [$C_4$mim]-$NTf_2$ Ionic Liquid. *J. Phys. Chem. B.* **2008**, *112*, 4357−4364.
(24) Tokuda, H.; Hayamizu, K.; Ishii, K.; Susan, M. A. B. H.; Watanabe, M. Physicochemical Properties and Structures of Room Temperature Ionic Liquids. 2. Variation of Alkyl Chain Length in Imidazolium Cation. *J. Phys. Chem. B.* **2005**, *109*, 6103−6110.
(25) Jiang, Y.; Blanchard, G. J. Rotational Diffusion Dynamics of Perylene in n-Alkanes. Observation of a Solvent Length-Dependent Change of Boundary Condition. *J. Phys. Chem.* **1994**, *98*, 6436−6440.
(26) Miyake, Y.; Hidemori, T.; Akai, N.; Kawai, A.; Shibuya, K.; Koguchi, S.; Kitazume, T. EPR Study of Rotational Diffusion in Viscous Ionic Liquids: Analysis by a Fractional Stokes−Einstein−Debye Law. *Chem. Lett.* **2009**, *38*, 124−125.